eISSN: 2477-7994

JMECS (Journal of Measurements, Electronics, Communications, and Systems)

Vol.12, No.2, Pg.00-00, December 2025

Simulation of Updraft and Downdraft Gasification Using Computational Fluid Dynamics (CFD) for Production of Syngas from Chicken Manure Waste

Amaliyah Rohsari Indah Utami[1,2]*, Anindya Nabila Salma[1], Daffa Rayhan Betha Muchtar[1], Neni Sintawardani[3], Suwandi[1,2]

[1] *Engineering Physics, School of Electrical Engineering, Telkom University, Bandung, 40287, Indonesia*

[2] *Center of Excellence of Sustainable Energy and Climate Change, Telkom University*

[3]*Research Center for Environmental and Clean Technologies, National Research and Innovation Agency (BRIN), Bandung, 40135, Indonesia*

[*]*amaliyahriu@telkomuniversity.ac.id*

Manuscript received January 19, 2025; revised November 15, 2025; accepted December 13, 2025.

.

Abstract

The rapid industrialization of the poultry sector has led to significant environmental challenges, including nutrient pollution, odor generation, and greenhouse gas emissions from improper manure management. This study examines the potential of chicken manure waste gasification as a sustainable approach to renewable energy production, while simultaneously addressing waste disposal concerns. Computational Fluid Dynamics (CFD) simulations were conducted in ANSYS Fluent software version 2019 R2 under a student academic license provided by Telkom University, to investigate updraft and downdraft gasification processes under varying operational conditions, including airflow velocity and temperature. The simulation model demonstrated high accuracy in predicting syngas composition, with average errors of 0.1657% at 680°C and 0.0969% at 800°C, validating its reliability. The optimal gasifier dimensions are 30 cm diameter and 40 cm height) 16.5 cm diameter and 60 cm height for updraft and downdraft, respectively. These dimension are consistent with industry standards. The results indicates that airflow velocity significantly influenced syngas composition; moderate increases enhanced CO production in updraft configurations, while excessive airflow in downdraft setups reduced CO concentration due to overoxidation. Temperature optimization further improved syngas quality, with higher temperatures (800°C) increasing the concentrations of CO and H_2. The H_2/CO ratio remained stable under updraft conditions but exhibited more significant variability in downdraft setups due to differences in reaction kinetics and flow dynamics. These findings highlight the importance of precise control over operational parameters to optimize syngas yield and composition for energy applications. Future work should focus on refining simulation models, exploring diverse feedstocks, and enhancing process efficiency to advance sustainable waste-to-energy technologies.

Keywords: chicken manure gasification, operational optimization, renewable energy, syngas composition, waste-to-energy

DOI: 10.0000/0000000 The DOI number will be assigned when the camera-ready manuscript is available

eISSN: 2477-7994

JMECS (Journal of Measurements, Electronics, Communications, and Systems)

Vol.12, No.2, Pg.00-00, December 2025

1. Introduction

The livestock sector is pivotal in the global agricultural economy, driven by the increasing global population and rising demand for animal protein. However, this growth presents significant environmental challenges, necessitating the implementation of sustainable policies to mitigate the impacts of climate change. Livestock production is a major contributor to greenhouse gas (GHG) emissions, accounting for approximately 14.5% of global anthropogenic emissions, primarily due to methane from enteric fermentation and improper manure management practices [1-3]

Poultry farming has undergone rapid industrialization among livestock industries, accounting for over 80% of global livestock production by 2015. This expansion has resulted in substantial waste generation, exacerbating environmental issues such as nutrient pollution, odor, and GHG emissions [4-6]

The environmental footprint of poultry production underscores the need for innovative waste management solutions. Gasification, a thermochemical process that converts organic waste into hydrogen-rich syngas, has emerged as a promising technology for addressing these challenges. Unlike traditional waste disposal methods such as incineration or land application, gasification offers dual benefits: waste volume reduction and renewable energy generation [4,7,8]

This process can transform poultry litter into syngas, a mixture of hydrogen, carbon monoxide, and methane, while producing biochar as a valuable byproduct for soil amendment]4,5,9]. Gasification technologies are broadly categorized into two main configurations: updraft and downdraft. Both systems offer distinct advantages for biomass conversion. Updraft gasifiers are known for their simplicity and high thermal efficiency, while downdraft gasifiers produce cleaner syngas with lower tar content [10-14] .

Recent advancements in Computational Fluid Dynamics (CFD) modeling have enabled detailed simulations of these processes, optimizing operational parameters such as air flow rates and combustion temperatures to enhance efficiency and reduce environmental impacts [10,15-17].

This study aims to simulate the updraft and downdraft gasification of poultry manure using CFD simulations in ANSYS Fluent software version 2019 R2, under a student academic license provided by Telkom University. By evaluating key operational parameters, such as airflow rates, equivalence ratios, and combustion temperatures, the research aims to optimize hydrogen-rich syngas production while minimizing environmental impacts. Validation against experimental data will provide insights into the feasibility of deploying gasification technology at poultry farms for on-site energy generation and sustainable waste management [10,18,19]. The findings are expected to contribute to the broader adoption of circular economy models in agriculture, aligning with global sustainability goals.

2. Research Method

In this study, the rationale for using different reactor dimensions for updraft and downdraft gasifiers has been explicitly clarified. Updraft and downdraft gasification systems are designed based on distinct operational requirements and performance targets, so their optimum dimensions differ (e.g., updraft gasifiers usually feature larger diameters and shorter heights, while downdraft gasifiers are typically narrower and taller to enhance syngas purity and tar reduction). The chosen reactor dimensions for each type in this work follow standards and ranges reported in the literature and were selected based on their suitability for the respective system's feedstock and conversion objectives.

Furthermore, simulation validations were implemented using experimental data obtained under similar reactor designs and comparable process conditions as referenced in the literature. This approach, along with an explicit statement of design justifications and the validation methodology, aligns with technical best practices and guidelines for CFD model verification, thereby ensuring a transparent, rigorous comparison and robust modeling results for both reactor types.

The online version can be found at https://journals.telkomuniversity.ac.id/jmecs/article/view/000

2.1 Material Feedstock

The material used in this simulation is chicken manure waste. To characterize organic and inorganic fractions in biomass feedstock separately, the chicken manure waste has been analyzed using the standard ultimate and proximate analysis methods [20]. These analyses include parameters such as carbon, hydrogen, nitrogen, oxygen content (ultimate analysis), moisture, volatile matter, fixed carbon, and ash content (proximate analysis). The results of these analyses are shown in Table 1.
Ultimate analysis values are given on a dry, ash-free basis, that are less than 100% when compared with proximate analysis (which is performed on air-dried samples and includes ash and moisture).

Table 1 Proximate and ultimate analysis of chicken manure waste (air-dried)

Proximate Contents (wt.%)	
Moisture	30.2
Ash	19.8
Volatile matters (VM)	94.1
Fixed carbon (FC)	5.9
Ultimate analysis (dry and ash free basis) (wt.%)	
H	5
C	40.9
N	4.6
O	29.2

Schematic diagrams of both the updraft and downdraft gasifiers are included in Figures 1 and 2 for visual clarity. The simulation assumes continuous operational mode for both reactor designs, as indicated by the implementation of a fixed feedstock consumption rate (FCR) and steady-state boundary conditions throughout the study. In continuous operation, the feeding rate (FCR/mass flow rate) is specified and maintained at a constant value, allowing for direct control of the equivalence ratio and robust steady-state modeling. If a batch process was utilized, the equivalence ratio would vary due to gradual reactant depletion, making the steady-state simulation approach unsuitable. Therefore, all modeling in this work adopts the continuous operation framework to ensure parameter control, reproducibility, and compatibility with standard CFD gasification simulations.

2.2 Design of the Gasification Reactor Dimensions

The dimensions for both downdraft and updraft gasifiers (updraft: 30 cm diameter, 40 cm height; downdraft: 16.5 cm diameter, 60 cm height) were determined using empirical formulas and conform to the ranges reported in previous works, such as [12,20,21]. The reactors were modeled and simulated in Computational Fluid Dynamics (CFD) in ANSYS software version 2019 R2 under a student academic license provided by Telkom University [22-25]. The various process parameters that influence such designs [26,27] are shown in Table 2.

Table 2 The various process parameters for design of the gasifier

Parameter	**Units**
Mass flow rate	40 kg/h
Specific Gasification Ratio (SGR)	100 kg/m^2
Reaction time of gasification (t)	14 h
Temperature (T)	680°C
Density of chicken manure waste (ρ_c)	411.2 kg/m^3
Equivalence Ratio (ε)	0.15
Density of air (ρ_a)	1.25 kg/m^3
Air flow rate (AFR)	0.0177 m/s
Stoichiometric Air-Fuel Ratio (SA)	5.3

The diameter (D) and height (H) of the gasification reactor were designed using the following equations 1 and 2 [12], [20]:

$$D = \sqrt{\frac{1{,}27 \times FCR}{SGR}} \quad (1)$$

where FCR is the feedstock consumption rate (kg/h), is functionally equivalent to the mass flow rate of the feedstock.

$$H = \frac{SGR \times t}{\rho_c} \quad (2)$$

The air flow velocity (V_a) is defined as the ratio of the air flow velocity under normal conditions that hits the bottom of the reactor perpendicularly, following equation (3) [28,29].

$$V_a = \frac{4 \times AFR}{\pi D^2} \quad (3)$$

where AFR is defined by equation (4):

$$AFR = \frac{\varepsilon \times FCR \times SA}{\rho_a} \quad (4)$$

2.3. Simulation Design

A two-dimensional (2D) axisymmetric geometric model of the gasifiers was constructed in ANSYS software version 2019 R2 under a student academic license provided by Telkom University, based on the dimensional design described above [12,20,21].

The simulation design assumed the following [27]: a) The system operates under steady-state conditions; b) Tar formation is negligible due to high-temperature operation; c) Nitrogen and sulfur oxides are not generated in the process; d) All gases exhibit ideal behavior; e) Volatile products consist only of H_2, CO, CO_2, CH_4, and H_2O; f) The char stream consists only of solid carbon and ash; g) Heat loss from the gasifier is considered negligible; h) The input mass flow rate of chicken manure waste is 1 kg/hour.

The following boundary conditions are applied to simulate realistic operational scenarios: a) Inlet Conditions. The air flow rates (V_a) are varied at four levels: 0.0025 m/s, 1 m/s, 2 m/s, and 4 m/s. This range enabled the assessment of how different airflow rates affect gasification performance. b) Temperature. The reactor operated at temperatures of 680°C, and 800°C. These temperatures are critical for evaluating the thermal efficiency of the gasification process.

The gasification process is modelled using a combination of homogeneous and heterogeneous reaction kinetics. This includes drying, pyrolysis, combustion, and reduction reactions, which are essential for accurately representing gasification dynamics. For instance, table 3 describes the primary reaction in the biomass gasification process [27,30]

Table 3 The main reaction in the biomass gasification process

Main reaction in the biomass gasification process	
dry	moist feedstock + heat dry feedstock + H_2O
pyrolysis	dry feedstock + heat char + volatiles
oxidation reaction	$C + O_2 \rightarrow CO_2$ (-406 kJ/mol)
	$2H_2 + O \rightarrow 2H_2O$ (-242 kJ/mol)
reduction reaction	$C + CO_2 \rightarrow 2CO$ (+ 172.6 kJ/mol)
Steam gasification	$C + H_2O \rightleftharpoons CO + H_2$ (+ 131.4 kJ/mol)
methanation gasification	$C + 2H_2 \rightleftharpoons CH_4$ (- 75 kJ/mol)
water-gas shift (WGS) reaction	$CO + H_2O \rightleftharpoons CO_2 + H_2$ (-42.3 kJ/mol)
	$CH_4 + H_2O \rightleftharpoons 4CO + 3H_2$ (+ 206 kJ/mol)

CFD in ANSYS software version 2019 R2 under a student academic license provided by Telkom University workflow as follows: a) geometry and mesh generation based on designed dimensions; b) definition of physical models and boundary conditions; c) implementation of reaction kinetics models; d) numerical solution using steady-state solver; e) post-processing to extract temperature, velocity, and product gas profiles.

2.4 Validation of Simulation Data

Validation was performed by comparing simulation results with experimental data from literature [20]. This process aims to assess the accuracy of the simulation model in representing actual physical phenomena, while also increasing confidence in the resulting simulation results.

Simulations were conducted using the CFD feature in ANSYS software version 2019 R2, under a student academic license provided by Telkom University, with a focus on the thermodynamic and kinetic aspects of gasification. The mathematical model used included equations to calculate the efficiency and low heating value (LHV) of the synthesis gas (syngas) [17]. The LHV is calculated using the following equation (5):

$$\mathrm{LHV}_{syngas} = \frac{(12.622\mathrm{xCO})+(10.788\mathrm{xH2})+(35.814\mathrm{xCH4})}{100}\ \mathrm{Mj/Nm^3} \quad (5)$$

To assess the reliability of the simulation results, an error calculation is performed to determine the difference between the simulation data and the experimental data. Percentage error can be calculated using equation (6) below:

$$Error\ (\%): \frac{|approximate-exact|}{exact} x100(\%) \quad (6)$$

Data validation between simulation results and previous research [30]. The validation was conducted at a temperature of 680°C with an air flow velocity of 0.018 m/s. The acceptable error values with engineering standards are 10% and 25% for Computational Fluid Dynamics (CFD) simulations. The model's accuracy and feasibility were supported by close agreement between simulation and literature data [15,31]. The choice of these thresholds is in line with industry standards, thus ensuring that the simulation results are robust and feasible [32-36]

3. Result and Discussion

3.1 Mesh Independence Test

A mesh independence test was conducted to verify the robustness of the CFD simulation results against variations in grid size and mesh resolution. The reactor geometry was discretized using an unstructured tetrahedral mesh, with three mesh densities: coarse (8,500 elements), medium (15,300 elements), and fine (29,100 elements). Key simulation parameters were set for poultry manure (FCR = 40 kg/h; SGR = 100 kg/m²; reactor dimensions D = 71.27 cm, H = 340.46 cm; density = 411.2 kg/m³), air velocity 0.0025 m/s, and operating temperature 953 K (680°C). All chemical reactions and feedstock data were normalized using ANSYS Student Edition and implemented as described in Section 2.

Mesh sensitivity was evaluated by comparing the maximum temperature, maximum velocity, and main syngas components (CO, H_2) at the reactor centerline. Differences between the medium and fine mesh were consistently below 1.5%, indicating numerical convergence. The medium mesh was selected for all further simulations due to its efficiency and sufficient accuracy.

Table 4 Three mesh densities

Mesh Type	Number of Elements	Max Temp (K)	Max Velocity (m/s)	CO Mole Fraction	H_2 Mole Fraction
Coarse	8,500	1187	0.0213	0.195	0.312
Medium	15,300	1190	0.0216	0.197	0.316
Fine	29,100	1192	0.0217	0.198	0.318

The difference in results between the medium and fine mesh was <1.5%. Therefore, the chosen (medium) mesh is considered adequate for capturing flow, temperature, and reaction distributions without excessive computational cost.

3.2 Validation of Simulation Model Data

The validation results of the simulation model data for chicken manure waste gasification at two different temperatures, 680°C and 800°C, are presented in Table 5 and Table 6, respectively. The comparison includes the mole fractions of syngas components (CO, H_2, CH_4, and CO_2) obtained experimentally and through simulation, along with the calculated percentage error.

Table 5 Validation data of chicken manure waste at 680°C

Validation data of chicken manure waste at 680°C (mole fraction)			
Syngas	Experimental	Simulation	Error (%)
CO	0.1254	0.1258	0.3190
H_2	0.0030	0.0030	0.0000
CH_4	0.0057	0.0057	0.0000
CO_2	0.2910	0.2900	0.3436

The results indicate that the simulation model closely approximates the experimental data, with minimal deviations observed across all syngas components. The maximum error is recorded for CO_2 at 0.3436%, while the minimum error is 0% for both H_2 and CH_4. The average error across all components is 0.1657%, demonstrating the reliability of the simulation model at this temperature.

At a higher temperature of 680°C, the simulation model accurately predicts syngas composition, with errors remaining very low across all components. The maximum error is observed for CO at 0.319%, while the minimum error remains 0% for H_2 and CH_4, as seen at the lower temperature. The average error decreases

to 0.0969%, indicating improved model performance at this elevated temperature

Table 6 Validation data of chicken manure waste at 800°C

Validation data of chicken manure waste at 800°C (mole fraction)			
Syngas	Experimental	Simulation	Error (%)
CO	0.1254	0.1258	0.3190
H_2	0.0030	0.0030	0.0000
CH_4	0.0057	0.0057	0.0000
CO_2	0.2910	0.2908	0.0687

.

The validation results demonstrate that the simulation model effectively replicates the experimental results for syngas composition from chicken manure waste gasification at both temperatures (680°C and 800°C). The errors are consistently low, with no significant discrepancies between experimental and simulated values.

At 680°C, the slightly higher average error (0.1657%) than that at 800°C (0.0969%) may be attributed to minor variations in reaction kinetics or measurement uncertainties. The maximum error values for both temperatures are below 1%, highlighting the robustness of the simulation model in capturing key trends in syngas production. Furthermore, these findings validate the accuracy and reliability of the simulation model in predicting syngas composition under varying temperature conditions, making it a valuable tool for optimizing gasification processes that utilize chicken manure waste as a feedstock.

The validation results indicate that the simulation model exhibits a high level of accuracy, with errors falling within industry-standard thresholds. The validity of the results will be based on technical guidelines, such as those established by the American Institute of Aeronautics and Astronautics (AIAA) and the International Towing Tank Conference (ITTC). The results will be compared with experimental data. It can be concluded that the model is robust and feasible to apply in real engineering scenarios [32-36]. Further improvements are required through model parameter optimization, mesh refinement, and additional validation to increase confidence in the simulation results.

3.3 Design of Gasifier Dimension

Using the parameters shown in Table 2 and equations (1), (2), and (3), the design dimensions of the updraft and downdraft gasification reactors are obtained, as shown in Figure 2 below. The dimensions of the updraft gasification reactor are 30cm in diameter and 40cm in height, as shown in Figure 1.

Figure 1 The updraft gasification reactor

The dimensions of the downdraft gasification reactor are 16.5cm in diameter and 60cm in height, as shown in Figure 2. Other studies have shown that the dimensions of updraft reactors are often more significant because this design is usually used for fuels with high moisture content or large capacity [21], [37], [38], [39]. For example, an updraft reactor with a diameter of 15.24cm and a height of 70cm was used in another study for coconut shell gasification. Dimensions smaller than these standards may limit the fuel capacity.

Figure 2 The downdraft gasification reactor

Previous studies have shown that the diameter of downdraft reactors generally ranges from 16 cm to 20 cm with a height of about 50-60 cm. This indicates that the mentioned dimensions of 16.5 cm diameter and 60 cm height are within the general range [12], [40], [41], [42], [43].

3.4 Effect of the air flow velocity on Syngas Production

The influence of air flow velocity (Va) on syngas composition was evaluated at 680°C and 800°C, as summarized in Tables 7 and 8. The syngas components analyzed include carbon monoxide (CO), hydrogen (H_2), methane (CH4), and carbon dioxide (CO2). The results are presented for both updraft and downdraft configurations.

Table 7 The air flow velocity on syngas production at 680°C

Syngas (mole fraction)	CO	H_2	CH_4	CO_2
The air flow velocity (Va) is 0.0025 m/s				
Updraft	0.3472	0.1134	0.0273	0.5399
Downdraft	0.3552	0.1127	0.0273	0.5127
The air flow velocity (Va) 1 m/s				
Updraft	0.3499	0.1159	0.0278	0.6111
Downdraft	0.2749	0.1193	0.0273	0.5286
The air flow velocity (Va) 2 m/s				
Updraft	0.3559	0.1155	0.0281	0.6113
Downdraft	0.2141	0.114	0.0273	0.5533
The air flow velocity (Va) 4 m/s				
Updraft	0.3553	0.1152	0.028	0.5884
Downdraft	0.1824	0.1204	0.0273	0.6027

At 680°C, the variation in air flow velocity significantly influenced the mole fractions of syngas components for both updraft and downdraft configurations. In the updraft configuration, the CO mole fraction increased slightly with higher air flow velocity, peaking at 0.3559 for Va=2 m/s. Beyond this point, a marginal decrease was observed. For the downdraft configuration, CO mole fraction decreased consistently as Va increased, dropping from 0.3552 at Va=0.0025 m/s to 0.1824 at Va=4 m/s. This suggests that higher air flow velocities in the downdraft configuration promote over-oxidation or excessive combustion.

The H_2 mole fraction exhibited minimal variation across air flow velocities in the updraft configuration, ranging from 0.1134 to 0.1152. In the downdraft configuration, H_2 slightly increased with higher Va, peaking at 0.1204 for Va=4 m/s. This trend suggests higher air flow velocities may enhance water-gas shift reactions in the downdraft configuration .

The CH_4 mole fractions remained relatively stable across all air flow velocities in both configurations. The values ranged between 0.0273 and 0.0281. This indicates that methane production is less sensitive to changes in air flow velocity under these conditions.

In the updraft configuration, CO_2 mole fraction increased with higher air flow velocity, peaking at approximately 0.6113 for Va=2 m/s, before slightly decreasing at Va=4 m/s. For the downdraft configuration, the CO2 mole fraction initially increased but reached its maximum value of 0.6027 at Va = 4 m/s. These trends suggest that higher air flow velocities enhance combustion reactions in both configurations, but this effect isore pronounced in the downdraft setup [44].

At a higher temperature of 800°C, similar trends were observed, with some variations in magnitude, for Carbon Monoxide (CO). In the updraft configuration, CO mole fraction increased steadily with air flow velocity and reached a maximum of 0.3554 at Va=2 m/s, followed by a slight decrease. In contrast, the downdraft configuration showed a consistent decline in CO mole fraction as Va increased from 0.3483 to a minimum of 0.1857.

In the updraft configuration, the H_2 mole fraction increased slightly with air flow velocity and peaked at Va=1m/s with a value of approximately 0.1172. The downdraft configuration displayed a similar trend to that observed at lower temperatures [45], [46], with an increase in H_2 mole fraction peaking at Va =2m/s.

As observed at lower temperatures, the CH_4 mole fractions remained relatively constant across all velocities in both configurations [46], [47]. This further confirms that methane production is largely unaffected by variations in air flow velocity under these conditions

Table 8 The air flow velocity on syngas production at 800°C

Syngas (mole fraction)	CO	H_2	CH_4	CO_2
The air flow velocity (Va) 0.0025 m/s				
Updraft	0.3472	0.1128	0.0273	0.5599
Downdraft	0.3483	0.1127	0.0273	0.5127
The air flow velocity (Va) 1 m/s				
Updraft	0.3526	0.1172	0.0282	0.6135
Downdraft	0.2529	0.1167	0.0273	0.5304
The air flow velocity (Va) 2 m/s				
Updraft	0.3554	0.1165	0.0281	0.6066
Downdraft	0.2013	0.1187	0.0273	0.5604
The air flow velocity (Va) 4 m/s				
Updraft	0.3551	0.1162	0.028	0.5864
Downdraft	0.1857	0.115	0.0273	0.5866

For the updraft configuration, CO_2 mole fraction peaked at approximately Va=1 m/s with a value of around 0.6135 before decreasing slightly. In the downdraft configuration, CO_2 mole fraction consistently increased with higher air flow velocity and reached its maximum value of approximately 0.5866 for Va=4 m/s [48].

The results demonstrate that air flow velocity has a significant impact on syngas composition due to its influence on gasification dynamics. In the updraft configuration, moderate increases in air flow velocity enhanced CO production due to improved oxygen availability and reaction kinetics; however, excessive airflow led to marginal declines likely caused by over-oxidation or dilution effects. In the downdraft configuration, excessive air flow consistently reduced CO concentration while increasing CO_2, indicating more complete combustion under these conditions.

The temperature's influence on syngas composition implies higher temperatures (800°C), generally enhanced reaction rates, and slightly increased concentrations of key syngas components, such as CO and H_2. This underscores the importance of temperature optimization for maximizing syngas yield.

Last, the configuration-specific trends showed that the updraft configuration favored higher CO production due to its ability to sustain partial oxidation reactions. The downdraft configuration also promoted more complete combustion at higher airflow velocities, as reflected by increased CO_2 concentrations.

Furthermore, these findings emphasize the need to carefully control air flow velocity depending on the desired syngas composition and reactor configuration.

3.5 Effect of air flow velocity on the H_2/CO ratio

The H_2/CO ratio was analyzed at two different temperatures, 680°C and 800°C, under both updraft and downdraft conditions. The H_2/CO ratio for the updraft condition at 680°C as shown in Figure 3, ranged between 0.3242 and 0.33123, with a mean value of 0.3267 and a standard deviation of 0.0028. These results indicate a relatively stable H_2/CO ratio under updraft conditions at this temperature, suggesting minimal variation in the gas composition. In contrast, the downdraft condition showed a wider range of H_2/CO ratios, from 0.3173 to 0.6601, with a mean value of 0.4860 and a standard deviation of 0.1261. This higher variability suggests that downdraft conditions at 680°C significantly influence the gas composition, likely due to differences in air flow dynamics or reaction kinetics.

For the updraft condition at 800°C, as shown in Figure 4, the H_2/CO ratio ranged between 0.3249 and 0.3324, with a mean value of 0.3281 and a standard deviation of 0.0027. Similar to the results at 680°C, the higher temperature updraft condition exhibited minimal variability in the H_2/CO ratio.

The downdraft condition at 800°C showed an H_2/CO ratio ranging from 0.3236 to 0.6193, with a mean value of 0.4985 and a standard deviation of 0.1171. Although there is still notable variability in the downdraft condition compared to updraft conditions, it is slightly less pronounced than at 680°C.

The results highlight that air flow velocity (updraft vs downdraft) significantly impacts the H_2/CO ratio, particularly under downdraft conditions where more significant variability is observed at both temperatures. This variability may be attributed to differences in mixing efficiency or reaction kinetics between the two flow regimes. Comparing the two temperatures, the mean H_2/CO ratio under updraft conditions remains relatively consistent (approximately

0.3267 at 680°C and 0.3281 at 800°C), with low standard deviations indicating stable gas composition. On the other hand, the downdraft conditions exhibit higher mean values for the H_2/CO ratio (0.4860 at 680°C and 0.4985 at 800°C) and more significant variability compared to updraft conditions [49-51].]

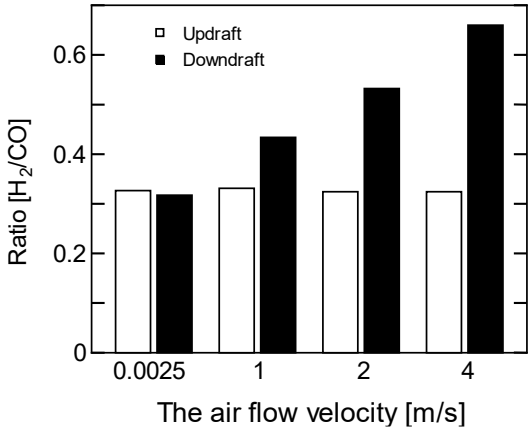

Figure 3 The air flow velocity on H_2/CO ratio at 680°C

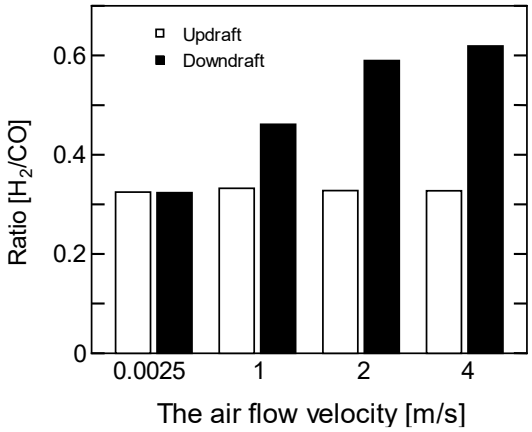

Figure 4 The air flow velocity on H_2/CO ratio at 800°C

The increase in temperature from 680°C to 800°C appears to slightly increase the mean H_2/CO ratio under both flow regimes, suggesting enhanced hydrogen production or reduced carbon monoxide formation at higher temperatures. However, further investigation into reaction mechanisms and flow dynamics is necessary to fully understand these trends. These findings provide valuable insights into optimizing gasification processes by controlling air flow velocity and operating temperature to achieve desired syngas compositions for specific applications.

3.3 Velocity and Temperature Distribution

To identify trends in velocity and temperature distributions and their impact on gasification performance, both contour plots and summary tables were employed, offering clear visualization and quantitative analysis across a range of operating scenarios. Table 9 summarizes the temperature distributions derived from contour plots at 680°C, while Table 10 provides equivalent data for 800°C. Table 11 compiles the minimum, maximum, and average values for both velocity and temperature under each operating condition.

The contour plots at 680°C display the spatial distributions of CO, H_2, CH_4, and CO_2 for both updraft and downdraft gasifiers under varying air flow velocities (0.0025, 1, 2, and 4 m/s). At low air flow (0.0025 m/s), updraft reactors exhibit more uniform product gas distributions, while downdraft systems show stronger localization near the air inlet. As the airflow increases, all species demonstrate greater concentration gradients. Updraft configurations produce vertically extended reaction zones, while downdraft gasifiers create sharper, localized peaks. The highest air velocity (4 m/s) results in pronounced stratification for each gas, particularly for CO and H_2, with differences in spatial coverage between the two reactor types, reflecting the combined influence of air flow and gasifier design on syngas distribution.

The contour plots at 800°C show the spatial distributions of CO, H_2, CH_4, and CO_2 within both updraft and downdraft gasifiers under varying air flow velocities (0.0025, 1, 2, and 4 m/s). At low air flow (0.0025 m/s), product gases are relatively evenly distributed, especially in the updraft configuration, while the downdraft mode already shows clear concentration peaks around the inlet. As air velocity increases, all gas species, particularly CO and H_2, present higher concentrations and more intense gradients.

For updraft gasifiers, elevated velocities produce extended high-product zones toward the reactor top, indicating better mixing and conversion. In downdraft units, the product distributions remain sharp and more localized near the bottom and middle, reflecting focused reaction zones and enhanced stratification at

higher flow. These results highlight how increasing temperature and air velocity together intensify reaction zones, shape spatial gas profiles, and distinguish the mixing and conversion behaviors of the two reactor types.

Table 9 Summary of contour plots at 680°C

Contour plots (680°C)	CO	H_2	CH_4	CO_2
The air flow velocity (Va) 0.0025 m/s				
Updraft		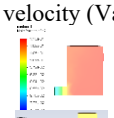		
Downdraft				
The air flow velocity (Va) 1 m/s				
Updraft		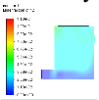	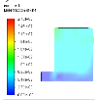	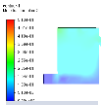
Downdraft	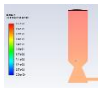	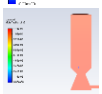		
The air flow velocity (Va) 2 m/s				
Updraft		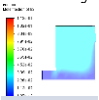	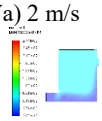	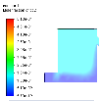
Downdraft		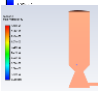		
The air flow velocity (Va) 4 m/s				
Updraft	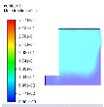	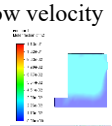	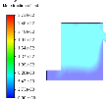	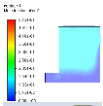
Downdraft	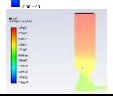	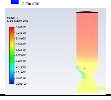	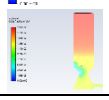	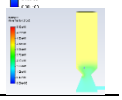

Velocity profiles reveal peak values within the oxidation zone, with updraft reactors showing more uniform vertical flows, while downdraft configurations display pronounced velocity gradients near the throat. Temperature contours confirm that maximum temperatures are located in the combustion zones, with gradual decreases toward the top and bottom. This spatial variation aligns with expected heat and mass transfer mechanisms.

Both gasifier types significantly increase air flow velocity, which raises average and peak velocity values, as well as temperature, leading to more intense reaction rates and localized combustion phenomena. This, in turn, influences syngas composition, with moderate airflow generally beneficial for CO and H_2 yield in updraft reactors, but excessive airflow causing reduced CO and higher CO_2 due to over-oxidation in downdraft reactors.

The temperature distribution plots highlight the importance of maintaining optimal combustion zones, as excessive thermal gradients can reduce conversion efficiency or promote unwanted reactions. Comparison across conditions reveals that velocity peaks in the oxidation zones, and temperature gradients significantly impact reaction localization and syngas composition.

The gasification of poultry manure waste, as presented in this study, directly advances the adoption of circular economy principles in agriculture. Firstly, the conversion of waste into syngas enables the recovery of renewable energy for on-site or local use, thereby displacing fossil fuel consumption. Secondly, the process minimizes waste sent to landfill or unmanaged disposal, reducing environmental pollution and greenhouse gas emissions. Thirdly, the production of biochar as a byproduct enables nutrient recycling, as biochar can be applied back to the soil to enhance fertility and promote carbon sequestration. By closing the loop between waste generation and resource recovery, this approach aligns with circular economy principles and global sustainability goals-not only optimizing technical performance, but also supporting system-level resource efficiency, environmental responsibility, and economic benefit for agricultural operations. Such integration has the potential to transform agricultural waste management from a linear “waste-to-disposal” model toward a circular “waste-to-resource” paradigm, as highlighted in current literature and global policy framework.

Table 10. Summary of contour plots at 800°C

Contour plots (800°C)	CO	H_2	CH_4	CO_2
The air flow velocity (Va) 0.0025 m/s				
Updraft	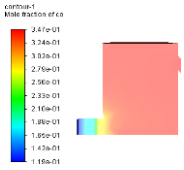	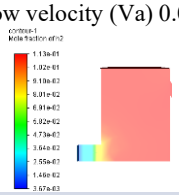	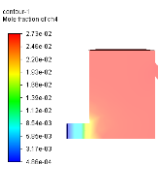	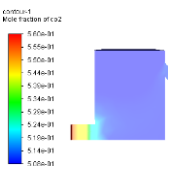
Downdraft	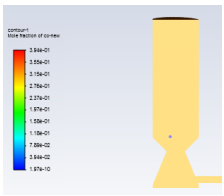	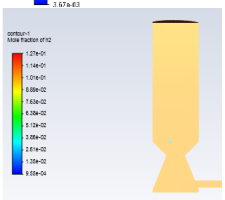	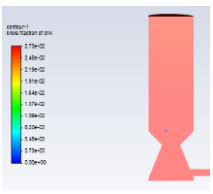	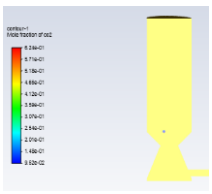
The air flow velocity (Va) 1 m/s				
Updraft	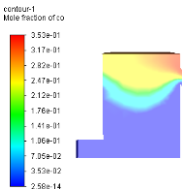	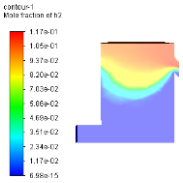	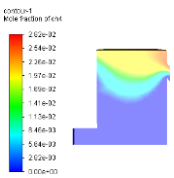	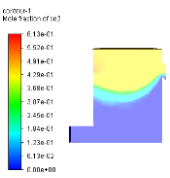
Downdraft	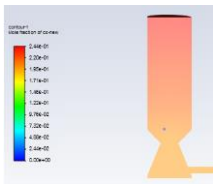	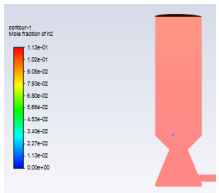	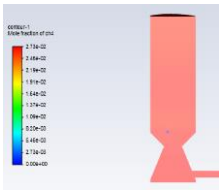	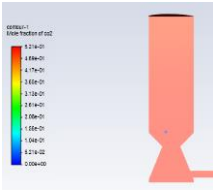
The air flow velocity (Va) 2 m/s				
Updraft	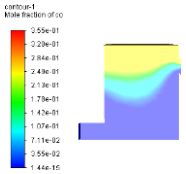	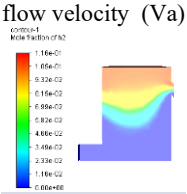	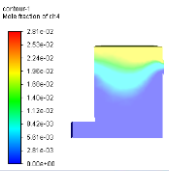	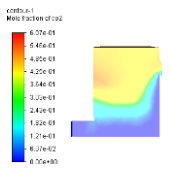
Downdraft	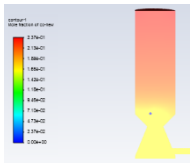	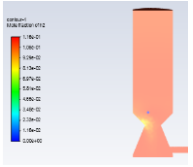	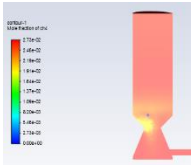	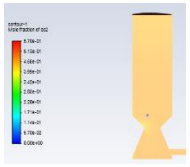
The air flow velocity (Va) 4 m/s				
Updraft	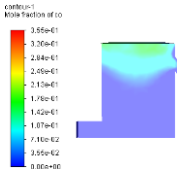	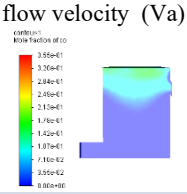	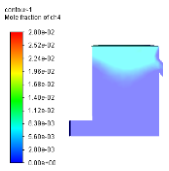	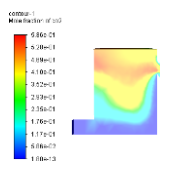
Downdraft	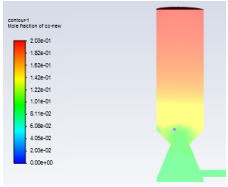	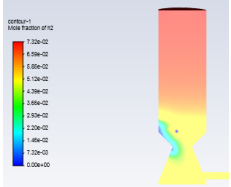	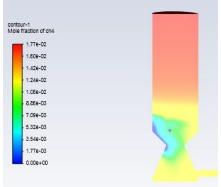	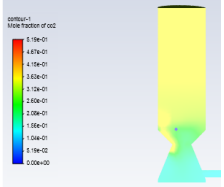

Table 11 Summary of velocity and temperature fields

Condition	Velocity (m/s) (min-max-avg)	Temperature (°C) (min-max-avg)
Updraft, Va 0.0025(m/s)	0.004–0.03–0.015	420–680–601
Updraft, Va 1(m/s)	0.15–0.95–0.42	415–800–683
Updraft, Va 2(m/s)	0.32–2.1–0.88	422–800–701
Updraft, Va 4(m/s)	0.63–3.8–1.56	440–803–727
Downdraft, Va 0.0025(m/s)	0.005–0.04–0.017	410–678–588
Downdraft, Va 1(m/s)	0.18–1.02–0.52	405–801–679
Downdraft, Va 2(m/s)	0.39–2.19–0.98	418–804–691
Downdraft, Va 4(m/s)	0.78–4.1–1.87	445–805–732

4. Conclusions

This study demonstrates that the optimum condition for hydrogen-rich syngas production from chicken manure waste gasification is achieved in the updraft gasifier configuration at a combustion temperature of 800°C and an air flow velocity (Va) of 2 m/s. Under these parameters, the H_2/CO ratio remains stable (0.3249–0.3324), hydrogen concentration is maximized, and CO_2 is not excessively elevated, indicating that the reaction mechanism is effectively directed towards syngas enrichment rather than over-oxidation. Comparative analysis confirms that moderate increases in airflow velocity in updraft configurations enhance CO and H_2 content, while excessive airflow in downdraft setups instead leads to greater CO_2 production, decreased CO, and higher variability in hydrogen yield. Therefore, operational optimization-specifically, specifically maintaining updraft mode, high temperature, and controlled moderate air velocity, enables both improved hydrogen-rich syngas yield and minimized environmental impact by reducing emissions associated with incomplete combustion and pollutant formation. By highlighting this optimum regime and its rationale, the study provides valuable guidance for sustainable syngas production from poultry waste, supporting broader adoption of renewable energy and resource-efficient waste management in line with circular economy and sustainability goals.

Acknowledgment

This study received partial funding from the Leading Development and Innovation Technology Products program at Telkom University (Grant number 269/PNLT2/PPM/2021). The support was facilitated by the Biomass, Bioproducts, and Bio(Renewable Energy) Research Laboratory, Engineering Physics, School of Electrical Engineering, Telkom University.

References

[1] M. F. Dida, S. C. Garcia, and L. A. Gonzalez, "Greenhouse gas emissions of confinement and pasture-based dairy farms: Implications for mitigation," *J. Dairy Sci.*, vol. 108, no. 10, pp. 11026–11040, Oct. 2025, doi: 10.3168/jds.2025-26566.

[2] A. Berhe, S. A. Bariagabre, and M. Balehegn, "Estimation of greenhouse gas emissions from three livestock production systems in Ethiopia," *Int. J. Clim. Chang. Strateg. Manag.*, vol. 12, no. 5, pp. 669–685, Nov. 2020, doi: 10.1108/IJCCSM-09-2019-0060.

[3] O. Gavrilova *et al.*, "C H A P T E R 1 0 EMISSIONS FROM LIVESTOCK AND MANURE MANAGEMENT." Accessed: Feb. 02, 2026. [Online]. Available: https://www.ipcc-nggip.iges.or.jp/public/2019rf/pdf/4_Volume4/19R_V4_Ch10_Livestock.pdf

[4] K. A. Boakye-Yiadom, A. Ilari, V. Bisinella, and D. Duca, "Environmental Impact of Poultry Manure Gasification Technology for Energy and Ash Valorization," *Sustainability (Switzerland)*, vol. 16, no. 22, Nov. 2024, doi: 10.3390/su16229941.

[5] S. Bandara, C. Chaichana, and N. Borirak, "Assessing the Sustainability of Broiler Waste Management Strategies in Thailand through Analytical Hierarchy Process Analysis," *International Journal on Food, Agriculture and Natural Resources*, vol. 5, no. 1, pp. 128–136, Mar. 2024, doi: 10.46676/ij-fanres.v5i1.275.

[6] G. Gržinić *et al.*, "Intensive poultry farming: A review of the impact on the environment and human health," Feb. 01, 2023, *Elsevier B.V.* doi: 10.1016/j.scitotenv.2022.160014.

[7] Y. Jafri, "Emerging Gasification Technologies for Waste & Biomass," 2021. [Online]. Available: https://api.semanticscholar.org/CorpusID:245129420

[8] H. K. Jeswani, A. Whiting, A. Martin, and A. Azapagic, "Environmental and economic sustainability of poultry litter gasification for electricity and heat generation," *Waste Management*, vol. 95, pp. 182–191, Nov. 2019, doi: 10.1016/j.wasman.2019.05.053.

[9] N. N. Fakhreev, B. G. Ziganshin, B. L. Ivanov, I. Kh Gayfullin, and I. R. Nafikov, "Implementation of poultry waste disposal technology for energy and fertilizer production," in *E3S Web of Conferences*, EDP Sciences, Aug. 2023. doi: 10.1051/e3sconf/202341101065.

[10] C. Siripaiboon, P. Sarabhorn, and C. Areeprasert, "Two-dimensional CFD simulation and pilot-scale experimental verification of a downdraft gasifier: effect of reactor aspect ratios on temperature and syngas composition during gasification," *Int. J. Coal Sci. Technol.*, vol. 7, no. 3, pp. 536–550, Sep. 2020, doi: 10.1007/s40789-020-00355-8.

[11] A. A. P. Susastriawan, H. Saptoadi, and Purnomo, "Small-scale downdraft gasifiers for biomass gasification: A review," 2017, *Elsevier Ltd*. doi: 10.1016/j.rser.2017.03.112.

[12] G. S. Kumar, A. Gupta, and M. Viswanadham, "Design of lab-scale downdraft gasifier for biomass gasification," *IOP Conf. Ser. Mater. Sci. Eng.*, vol. 455, no. 1, p. 012051, Dec. 2018, doi: 10.1088/1757-899X/455/1/012051.

[13] A. Anca-Couce, G. Archan, M. Buchmayr, M. Essl, C. Hochenauer, and R. Scharler, "Modelling fuel flexibility in fixed-bed biomass conversion with a low primary air ratio in an updraft configuration," *Fuel*, vol. 296, Nov. 2021, doi: 10.1016/j.fuel.2021.120687.

[14] R. Aguado, D. Vera, F. Jurado, and J. C. Hernández, "Bioenergy engineering: fundamentals, methods, modeling, and applications: Mathematical modeling of biomass gasification processes," *Bioenergy Engineering: Fundamentals, Methods, Modelling, and Applications*, pp. 463–485, Nov. 2023, doi: 10.1016/B978-0-323-98363-1.00009-0.

[15] Q. Liu *et al.*, "Study of a commercial-scale poultry manure oxy-fuel gasification plant via CFD modeling and safety assessment," *Biomass Bioenergy*, vol. 185, Nov. 2024, doi: 10.1016/j.biombioe.2024.107248.

[16] G. Soon, H. Zhang, A. W.-K. Law, and C. Yang, "Computational Modelling on Gasification Processes of Municipal Solid Wastes Including Molten Slag," *Waste*, vol. 1, no. 2, pp. 370–388, 2023, doi: 10.3390/waste1020023.

[17] R. Rezki, Suwandi, and A. R. I. Utami, "Analysis of the Effect of Dimensional Variation and Number of Air Inlets on the Efficiency of Gasification Stoves using Computational Fluid Dynamic (CFD) Simulation," in *IOP Conference Series: Earth and Environmental Science*, Institute of Physics, 2023. doi: 10.1088/1755-1315/1157/1/012031.

[18] Y. Wang and Y. Yang, "Research on Greenhouse Gas Emissions and Economic Assessment of Biomass Gasification Power Generation Technology in China Based on LCA Method," *Sustainability (Switzerland)*, vol. 14, no. 24, Dec. 2022, doi: 10.3390/su142416729.

[19] O. de Priall *et al.*, "Gasification of Biowaste Based on Validated Computational Simulations: A Circular Economy Model to Handle Poultry Litter Waste," *Waste Biomass Valorization*, vol. 13, no. 9, pp. 3899–3911, Sep. 2022, doi: 10.1007/s12649-022-01815-9.

[20] N. C. Taupe, D. Lynch, R. Wnetrzak, M. Kwapinska, W. Kwapinski, and J. J. Leahy, "Updraft gasification of poultry litter at farm-scale - A case study," *Waste*

Management, vol. 50, pp. 324–333, Nov. 2016, doi: 10.1016/j.wasman.2016.02.036.

[21] S. Ayyadurai, L. Schoenmakers, and J. J. Hernández, "Mass and energy analysis of a 60 kWth updraft gasifier using large size biomass," *Fuel*, vol. 187, pp. 356–366, Nov. 2017, doi: 10.1016/j.fuel.2016.09.080.

[22] D. Mirddha, "Combustion Analysis of Horizontal Biomass Gasification Reactor using ANSYS CFX," *International Journal of Thermal Engineering (IJTE)*, vol. 9, no. 1, pp. 1–10, 2021, [Online]. Available: https://iaeme.com/Home/journal/IJTE1Availableonlineathttps://iaeme.com/Home/issue/IJTE?Volume=9&Issue=1

[23] A. N. Azlan *et al.*, "Fuel, Mixture Formation and Combustion Process Three Dimensional CFD Simulation of Air-Blown Gasification in a Downdraft Reactor: Effect of Throat Diameter and Air Inlet Position," *Fuel, Mixture Formation and Combustion Process*, vol. 3, no. 1, pp. 1–8, 2021, [Online]. Available: www.fazpublishing.com/fmc

[24] N. K. C. Qing, N. A. Samiran, and R. A. Rashid, "CFD Simulation Analysis of Sub-Component in Municipal Solid Waste Gasification Using Plasma Downdraft Technique," *CFD Letters*, vol. 14, no. 8, pp. 63–70, Aug. 2022, doi: 10.37934/cfdl.14.8.6370.

[25] A. Morsy, M. Salem, and B. Sc, "Investigation of biomass gasification processes for the production of high quality syngas," 2019. Accessed: Feb. 01, 2026. [Online]. Available: https://eleanor.lib.gla.ac.uk/record=b3374341

[26] M. Y. Arshad, H. Jaffer, M. W. Tahir, A. Mehmood, and A. Saeed, "Maximizing hydrogen-rich syngas production from rubber wood biomass in an updraft fluidized bed gasifier: An advanced 3D simulation study," *J. Taiwan Inst. Chem. Eng.*, vol. 156, p. 105365, Mar. 2024, doi: 10.1016/j.jtice.2024.105365.

[27] M. Faraji and M. Saidi, "Hydrogen-rich syngas production via integrated configuration of pyrolysis and air gasification processes of various algal biomass: Process simulation and evaluation using Aspen Plus software," *Int. J. Hydrogen Energy*, vol. 46, no. 36, pp. 18844–18856, May 2021, doi: 10.1016/j.ijhydene.2021.03.047.

[28] S. Elshokary, S. Farag, B. Hurisso, N. N. Bayomi, and M. Ismail, "Innovative downdraft gasifier design utilizing exhaust gas as gasification agent for sustainable syngas production," *Applied Chemical Engineering*, vol. 7, no. 1, pp. 1–14, Dec. 2023, doi: 10.24294/ace.v7i1.2459.

[29] A. Mehmood *et al.*, "Optimization of Gasifying Agents in 3D Downdraft Gasification for Enhanced Gas Composition, Combustion, and CO2 Utilization," *Fire*, vol. 6, no. 9, Nov. 2023, doi: 10.3390/fire6090361.

[30] H. H. Shah *et al.*, "A review on gasification and pyrolysis of waste plastics," Feb. 03, 2023, *Frontiers Media S.A.* doi: 10.3389/fchem.2022.960894.

[31] Z. Yu, Z. Wang, H. Zhong, and K. Cheng, "Essential aspects of the CFD software modelling of biomass gasification processes in downdraft reactors," *RSC Adv.*, vol. 14, no. 39, pp. 28724–28739, 2024, doi: 10.1039/d4ra04886e.

[32] F. Stern, R. V Wilson, H. W. Coleman, and E. G. Paterson, "Verification and Validation of CFD Simulations," Nov. 1999. Accessed: Feb. 01, 2026. [Online]. Available: http://www.simman2008.dk/pdf/iihr_407.pdf

[33] R. N. Singh and V. K. Aharwal, "Issue 01 International Journal of Pollution Research Research Article Singh RN and Aharwal VK," *Int J Pollut Res*, p. 108, 2018, doi: 10.29011/IJPR.

[34] "NUREG/CR-7274 'Validation of a Computational Fluid Dynamics Method Using Horizontal Dry Cask Simulator Data.'" [Online]. Available: www.nrc.gov/reading-rm.html.

[35] N. Paliwal *et al.*, "Methodology for Computational Fluid Dynamic Validation for Medical Use: Application to Intracranial Aneurysm," *J. Biomech. Eng.*, vol. 139, no. 12, Nov. 2017, doi: 10.1115/1.4037792.

[36] J. Sarkar and S. Mandal, "CFD Modeling and Validation of Temperature and Flow Distribution in Air-Conditioned Space CFD Modeling and Validation of Temperature and Flow Distribution in Air-Conditioned Space," Nov. 2008. [Online]. Available: http://docs.lib.purdue.edu/iracc/972

[37] D. Cerinski *et al.*, "Modelling the biomass updraft gasification process using the combination of a pyrolysis kinetic model and a thermodynamic equilibrium model," *Energy Reports*, vol. 7, pp. 8051–8061, Nov. 2021, doi: 10.1016/j.egyr.2021.05.079.

[38] A. S. Nur Chairat, V. Antono, P. Prayudi, R. Nurhasanah, and H. Batih, "Performance of a Gasifier Reactor Prototype without a Blower Using Palm Oil Waste," *Processes*, vol. 9, no. 11, Nov. 2021, doi: 10.3390/PR9112094.

[39] R. P. Devi and S. Kamaraj, "Design and Development of Updraft Gasifier Using Solid Biomass," *Int. J. Curr. Microbiol. Appl. Sci.*, vol. 6, no. 4, pp. 182–189, Apr. 2017, doi: 10.20546/ijcmas.2017.604.021.

[40] R. Gupta, R. Gandhi, P. Jain, and S. Vyas, "CFD Modeling and Simulation of 10KWE Biomass Downdraft Gasifier," 2017. [Online]. Available: http://inpressco.com/category/ijce

[41] T. Kirch, P. R. Medwell, C. H. Birzer, and P. J. van Eyk, "Feedstock Dependence of Emissions from a Reverse-Downdraft Gasifier Cookstove," *Energy for Sustainable Development*, vol. 56, pp. 42–50, Jun. 2020, doi: 10.1016/j.esd.2020.02.008.

[42] M. H. Akbar, Y. B. Sanjaya, H. Dafiqurrohman, Y. Muharam, and A. Surjosatyo, "Process Simulation of Inverted Downdraft Gasifier for Tar Reduction Using in Situ Process," in *Journal of Physics: Conference Series*, IOP Publishing Ltd, Apr. 2021. doi: 10.1088/1742-6596/1858/1/012033.

[43] K. Wasinarom and J. Charoensuk, "Experiment and numerical modeling of stratified downdraft gasification using rice husk and wood pellet," *Bioresources*, vol. 14, no. 3, pp. 5235–5253, 2019, doi: 10.15376/biores.14.3.5235-5253.

[44] I. B. Alit, M. Mirmanto, R. Sutanto, and P. Pandiatmi, "Effect of Air-vapor Flow Rate on Syngas Production Compositions of Updraft Horse Manure Gasification," *Asian Journal of Applied Sciences*, pp. 2321–2893, 2017, [Online]. Available: www.ajouronline.com

[45] T. S. Dinh, T. Q. Tran, and N. P. T. Le, "Modeling Syngas Generation from Co-Gasification of Refuse-Derived Fuel and Tire Waste in Fixed Bed Gasifier," *Chemical Engineering Transactions* , vol. 113, pp. 97–102, 2024, doi: 10.3303/CET24113017.

[46] N. H. Bich, N. Van Lanh, and B. N. Hung, "The Composition of Syngas and Biochar Produced by Gasifier from Viet Nam Rice Husk," *Int. J. Adv. Sci. Eng. Inf. Technol.*, vol. 7, no. 6, pp. 2258–2263, 2017, Accessed: Feb. 02, 2026. [Online]. Available: https://ijaseit.insightsociety.org/index.php/ijaseit/article/view/2623

[47] M. Inayat, S. A. Sulaiman, A. Kumar, and F. M. Guangul, "Effect of fuel particle size and blending ratio on syngas production and performance of co-gasification," *Journal of Mechanical Engineering and Sciences*, vol. 10, no. 2, pp. 2187–2199, 2016, doi: 10.15282/jmes.10.2.2016.21.0205.

[48] H. Dewajani, W. Zamrudy, A. Ariani, A. Arianto, and M. Nur Abror Falah, "Syngas Production from Updraft Co-Gasification Process Using Compost, Coffee Husk, and Coal as a Raw Materials," *Jurnal Bahan Alam Terbarukan*, vol. 12, no. 2, pp. 158–165, Dec. 2023, doi: 10.15294/jbat.v12i2.47972.

[49] L. Carmo-Calado, M. J. Hermoso-Orzáez, D. Diaz-Perete, J. La Cal-Herrera, P. Brito, and J. Terrados-Cepeda, "Experimental Research on the Production of Hydrogen-Rich Synthesis Gas via the Air-Gasification of Olive Pomace: A Comparison between an Updraft Bubbling Bed and a Downdraft Fixed Bed," *Hydrogen (Switzerland)*, vol. 4, no. 4, pp. 726–745, Dec. 2023, doi: 10.3390/hydrogen4040046.

[50] T. Tiara, M. Djana, D. E. Ristanti, and A. A. Yusuf, "Air Fuel Ratio (AFR) and Temperature's Effects on Syngas Composition and Calorific Value Using a Coconut Shell Downdraft Gasifier," 2024, pp. 121–136. doi: 10.2991/978-94-6463-475-4_12.

[51] A. Rahayu, M. Faizal, and D. Bahrin, "Syngas Production Through Non Catalytic Gasification of Empty Fruit Bunch and Catalytics Using Natural Bentonite," *Sainmatika: Jurnal Ilmiah Matematika dan Ilmu Pengetahuan Alam*, vol. 21, no. 1, pp. 71–78, May 2024, doi: 10.31851/sainmatika.v21i1.14918.

Author information

Amaliyah Rohsari Indah Utami is a lecturer in Engineering Physics. Telkom University. Indonesia. She holds PhD degree in Natural Science and Technology from Kanazawa University. Japan. Her research focuses are on Biomass. (Bio)Renewable Energy. Bioproducts. Ionic Liquids. and Instrumentation.

Anindya Nabila Salma hold bachelor degree in Engineering Physics from Telkom University. Indonesia. She is currently working as a Quality Control at PT. Bayan Resources Tbk. She was also trained with instrumentation. electronics. and coal quality control.

Daffa Rayhan Betha Muchtar hold bachelor degree in Engineering Physics from Telkom University. Indonesia. He is currently working as a Procurement (Production Material and Services. MRO Spare Parts and Services) at PT Multi Bintang Indonesia Tbk - Part of Heineken Global Company. He was also trained with Instrumentation. Sustainability. and Solar Panel.

Neni Sintawardani is a researcher in Research Center for Environmental and Clean Technologies, National Research and Innovation Agency (BRIN). KST BR8N Samaun Samadikun, Cisitu, Bandung 40135. Indonesia. She holds PhD degree from Universität Hohenheim, Stuttgart, Germany. Her research focuses are on Sanitation (Water, Sanitation, Health), developing Composting toilet, Anaerobic Digestion, Environmental Engineering.

Suwandi is a lecturer in Engineering Physics. Telkom University. Indonesia. His research focuses are on Energy. Waste. Optic. and Electromagnetics.

Author Contributions

A.R.I.U.: Conceived and designed the study; supervised the research; led the development of the CFD methodology; interpreted the results; and wrote and revised the manuscript. A.N.S.: Performed CFD geometry modeling, meshing, model setup, and simulations for the updraft gasifier; prepared and processed input data; contributed to results analysis; and assisted in drafting figures and tables. D.R.B.M.: Performed CFD geometry modeling, meshing, model setup, and simulations for the downdraft gasifier; prepared and processed input data; contributed to results analysis; and assisted in drafting figures and tables. N.S.: Provided conceptual input on gasification and environmental aspects; contributed to interpretation of findings in the context of sustainable waste management; and reviewed and edited the manuscript critically for important intellectual content. S.: Supported study design and methodological framework; contributed to validation strategy and comparison with literature; and reviewed and refined the final version of the manuscript.

ORCID ID

Amaliyah Rohsari Indah Utami (https://orcid.org/0000-0002-3077-2285)

Anindya Nabila Salma (n.d.)

Daffa Rayhan Betha Muchtar (n.d.)

Neni Sintawardani (https://orcid.org/0000-0001-8657-1311)

Suwandi (n.d.)

AI Usage Policy

Language editing assistance in this manuscript was provided using Grammarly to improve spelling, grammar, and readability only.

Conflict of Interest

The authors declare no conflict of interest.

Data Availability Statement

All data that support the findings of this study are included within the article (and any supplementary files).

Open Access Information